◼ 1006

State-space averaged modeling and transfer function derivation of DC-DC boost converter for high-brightness led lighting applications

Muhammad Wasif Umar*, Norzaihar Yahaya, Zuhairi Baharudin
Department of Electrical and Electronic Engineering, Universiti Teknologi PETRONAS
32610, Bandar Seri Iskandar, Perak, Malaysia
*Corresponding Author, e-mail: cmwasif@yahoo.com

Abstract

This paper presents dynamic analysis of a boost type DC-DC converter for high-brightness LED (HBLED) driving applications. The steady state operation in presence of all system parasitics has been discussed for continuous conduction mode (CCM). The state-space averaging, energy conservation principle and standard linearization are used to derive ac small signal control to inductor current open-loop transfer function of the converter. The derived transfer function can be further used in designing a robust feed-back control network for the system. In the end frequency and transient responses of the derived transfer function are obtained for a given set of component values, hence to provide a useful guide for control design engineers.

Keywords: averaged modeling, continuous conduction mode (CCM), control transfer function, DC-DC boost converter, high-brightness LEDs, parasitic elements, state-space averaging

1. Introduction

Since the advent of high-brightness light emitting diodes *(HB-LEDs),* driving them has been a matter of great research. They are current operated semiconductor devices having electrical characteristics completely different to their traditional counterparts *(Halogen and HID)* [1, 2]. The output luminous flux of a high-brightness LED is direct function of its forward current hence cannot be powered by using conventional driving schemes. Their driving systems must be capable of providing constant LED current while maintaining the required level of luminance [3-8].

Switch mode converters offer a convenient solution to power high-brightness LEDs and control their luminance in a wide range of applications [9]. In order to achieve the required values of current and voltage these converters rely on control networks. For an adequate controller design, accurate analytical model based knowledge of converter power stage is essential [10, 11]. However, analytical modeling of these converters presents significant challenges. Such systems comprise of linear (inductor *L*, capacitor *C* and resistor *R*) and nonlinear (switch *S*) components making them nonlinear time-variable circuits.

The purpose of this paper is to introduce model based analytical solution of a boost type dc-dc converter for high-brightness LED lighting applications. To achieve the high accuracy and greater design flexibility all the system parasitics have been taken into account in modeling process. Finally, small signal ac control to inductor current transfer function has been obtained and various bode diagrams are plotted to illustrate the frequency and transient response. The results obtained can be further used to obtain a linear current-mode controller circuit for system-level studies.

2. Switching Converter Control Design using Modeling

As mentioned earlier in order to design a suitable control circuit for LED driving, one must have analytical based knowledge of system behaviour. It involves physical knowledge of the system in terms of mathematical and mass and energy conservation laws. Standard methods of analytical modeling, namely state-space averaging *(SSA)* and circuit averaging *(CA)* are widely

described in the literature [10-14]. However, state-space averaging is a well-known standard for modelling electronic systems in system-level studies. A switching power converter normally operates in two different modes of operation depending on the state of the respective semiconductors. Considering all the power semiconductors as ideal or loss-less, then the circuit behavior in term of time t over time period T can be wirtten in general state-space form by a set of two vectorial [10-13]. Here, x and u represent state and control vectors respectively whereas coefficient of the matrices A, B, C and D are function of the circuit elements. These matrices depend on the converter topology and characteristics of its components.

$$\left.\begin{array}{l} \dfrac{dx}{dt} = \overset{\bullet}{x} = Ax + Bu \\ y = Cx + Du \end{array}\right\} \tag{1}$$

3. System Description and Modeling

Studies show that the output luminous flux of a high-brightness LED is determined by its forward current [4-6, 15]. The electrical characteristics of high-brightness LEDs resemble that of a voltage source and they are unable to regulate their own current. Therefore, for an accurate driving system model it is necessary to take into account the behavioural model of the LED load in the modeling process as well. The linear representation of a high brightness LED can be seen in Figure 1 which contains a source voltage which is the threshold voltage V_F, and R_S series resistance that represents the dynamic resistance of the LED.
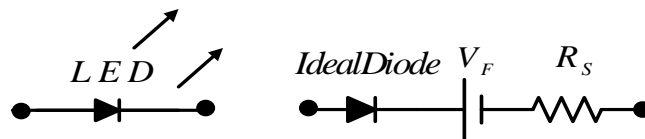

Figure 1. Linear representation of LED

Then, the LED voltage equation can be represented as:

$$V_{LED} = V_F + I_F R_S \tag{2}$$

Thus, it is crucial to determine the type of LED load that complies with the requirements of the application under consideration. In this work we considered an automotive headlamp with *LUXEON Rebel ES* high brightness LEDs as load. A dc-dc boost converter has been selected as candidate for the driver circuit. Boost is a popular non-isolated switched-mode topology capable of producing dc output voltage greater in magnitude than the input voltage. A typical boost power stage consists of an inductor *L*, a controllable switch *S (MOSFET, BJT, or IGBT)*, a diode *D* and an output capacitor *C* and as shown below in Figure 2. The desired output regulation is achieved by changing the duty cycle *d* or on-time of the switch *S*. Usually, this duty cycle control is generated by using a modulation technique such as pulse width modulation *(PWM)*.

The above is an ideal representation of boost power stage; however in realty it has some system parasitics such as equivalent series resistances (ESR) of inductor and capacitor. The idea of simply considering ideal/lossless components is to simplify the modeling process and understanding the fundamental behavior of the sysytem. But this is not a good approach, because it does not represent the actual dynamic behavior of the system. Therefore, to increase the model accuracy all circuit parasitic elements should be considered in modeling process [16]. Figure 3 shows an equivalent circuit of boost power stage with circuit parasitics.
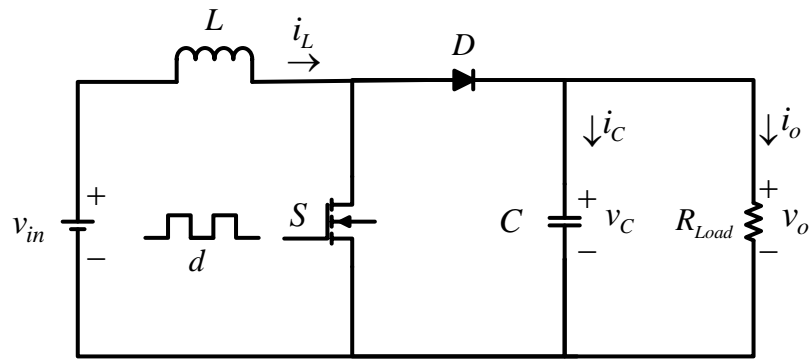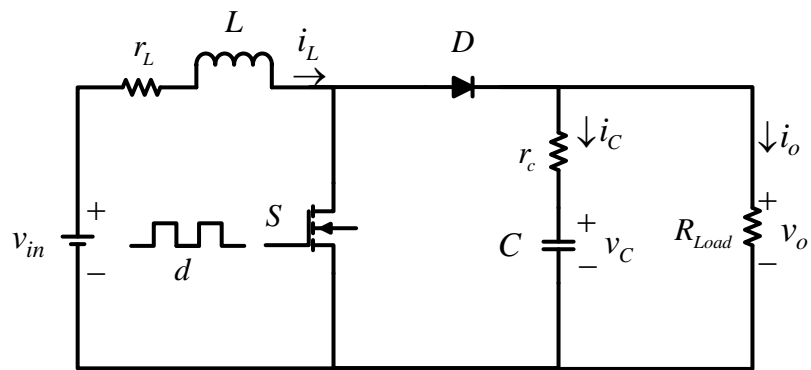
Figure 2. Boost converter circuit

Figure 3. Boost converter with circuit parasitic elements

Here r_L and r_C represent the inductor and capacitor equivalent series resistances (*ESR*) while both the switches have almost neglible turn on resistances. If it is assumed that the converter is operating in continuous conduction mode (*CCM*) then in one switching cycle it will exhibit two modes of operation depending on the '*ON*' and '*OFF*' time of the switch *S*. The on-time (t_{ON}) can be defined in terms of duty cycle d by dTs, and off-time (t_{OFF}) by $(1-d)Ts$. Whereas duty cycle d is determined by the pulse generator over time period Ts of one switching cycle as shown in Figure 4 [13].
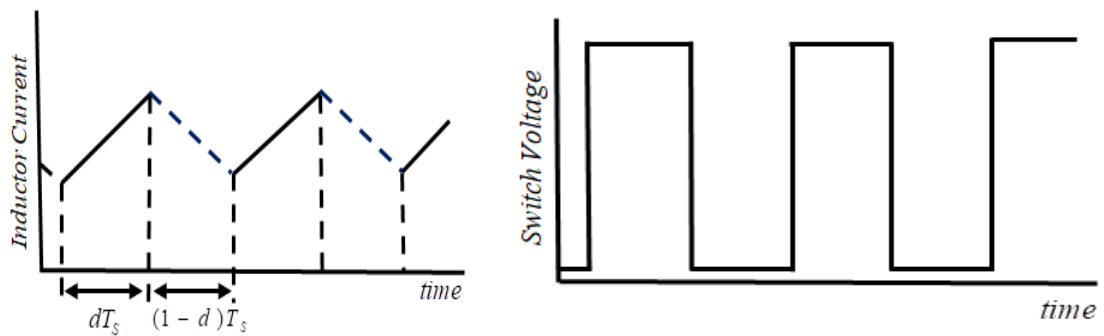

Figure 4. Steady-state inductor current in CCM and corresponding switch voltage

The system can be described over one complete switching cycle by employing state-space averaging as given below:

$$\text{'ON' Mode} \quad \begin{cases} \dfrac{dx}{dt} = \overset{\bullet}{x} = A_1 x + B_1 v_{in} \\[2mm] y = C_1 x \end{cases} \tag{3}$$

$$\text{'OFF' Mode} \quad \begin{cases} \dfrac{dx}{dt} = \overset{\bullet}{x} = A_2 x + B_2 v_{in} \\[2mm] y = C_2 x \end{cases} \tag{4}$$

Where A_1, B_1, C_1 represent the state matrices for 'ON' mode and A_2, B_2, C_2 for 'OFF' mode respectively.

3.1. 'ON' Mode: $0 \le t \le dTs$
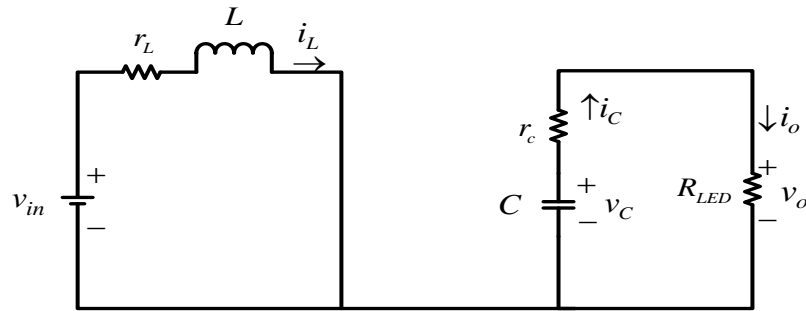When the switch S is 'ON' the system can be represented as in Figure 5.

Figure 5. Equivalent circuit during 'ON' state

State equations for *'ON'* mode can be written by using Kirchhoff's voltage law *(KVL)*

$$L\frac{di_L}{dt} = v_{in} - r_L * i_L \tag{5}$$

$$C\frac{dv_c}{dt} = -\frac{v_c}{R_{LED} + r_c} \tag{6}$$

$$v_o = \frac{R_{LED} v_c}{R_{LED} + r_c} \tag{7}$$

Taking i_L and v_C as state variables the state-space matrix form can be obtained:

$$\begin{bmatrix} \dfrac{di_L}{dt} \\[3mm] \dfrac{dv_c}{dt} \end{bmatrix} = \begin{bmatrix} \dfrac{-r_L}{L} & 0 \\[3mm] 0 & \dfrac{-1}{C(R_{LED} + r_c)} \end{bmatrix} \begin{bmatrix} i_L \\ v_c \end{bmatrix} + \begin{bmatrix} \dfrac{1}{L} \\[2mm] 0 \end{bmatrix} v_{in} \tag{8}$$

$$v_o = \begin{bmatrix} 0 & \dfrac{R_{LED}}{R_{LED} + r_c} \end{bmatrix} \begin{bmatrix} i_L \\ v_c \end{bmatrix}$$

$$(9)$$

3.2. 'OFF' Mode: $dTs < t \le Ts$

Similarly when the switch *S* is '*OFF*' the state equations for system shown in Figure 6 can be written as:
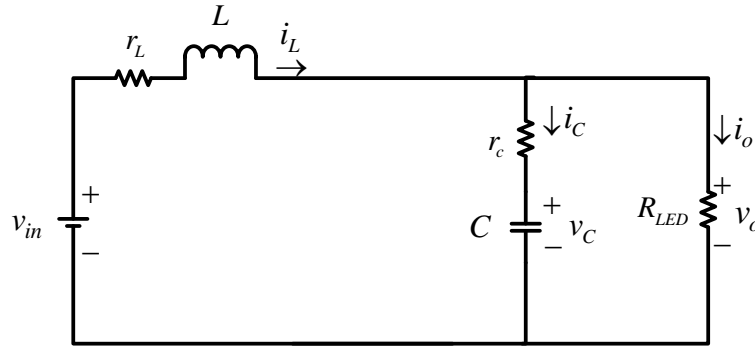

Figure 6. Equivalent circuit during '*OFF*' state

$$L\frac{di_L}{dt} = v_{in} - r_L * i_L - v_o$$

$$(10)$$

$$C\frac{dv_c}{dt} = \frac{R_{LED}}{R_{LED} + r_c} i_L - \frac{v_c}{R_{LED} + r_c}$$

$$(11)$$

$$v_o = \frac{R_{LED}r_c}{R_{LED} + r_c} i_L + \frac{R_{LED}v_c}{R_{LED} + r_c}$$

$$(12)$$

The state-space matrix form can be described as:

$$\begin{bmatrix} \dfrac{di_L}{dt} \\ \dfrac{dv_c}{dt} \end{bmatrix} = \begin{bmatrix} \left[\left(\dfrac{-r_L}{L}\right) - \left(\dfrac{R_{LED}r_c}{L(R_{LED} + r_c)}\right)\right] & \dfrac{-R_{LED}}{L(R_{LED} + r_c)} \\ \dfrac{R_{LED}}{C(R_{LED} + r_c)} & \dfrac{-1}{C(R_{LED} + r_c)} \end{bmatrix} \begin{bmatrix} i_L \\ v_c \end{bmatrix} + \begin{bmatrix} \dfrac{1}{L} \\ 0 \end{bmatrix} v_{in}$$

$$(13)$$

$$v_o = \begin{bmatrix} \dfrac{R_{LED}r_c}{R_{LED} + r_c} & \dfrac{R_{LED}}{R_{LED} + r_c} \end{bmatrix} \begin{bmatrix} i_L \\ v_c \end{bmatrix}$$

$$(14)$$

Employing circuit averaging

$$\left. \begin{aligned} x' &= \left[A_1 d + A_2(1-d)\right]\overline{x} + \left[B_1 d + B_2(1-d)\right]v_{in} \\ y' &= \left[C_1 d + C_2(1-d)\right]\overline{x} \end{aligned} \right\}$$

$$(15)$$

and the parameters *A,B* and *C* can be further solved as follows:

$$A = \left[A_1 d + A_2 (1-d) \right]$$

(16)

Hence, the statespace averaged model for the converter operating in *CCM* and including all system parasitics can be represented as:

$$\begin{bmatrix} \dfrac{di_L}{dt} \\ \dfrac{dv_c}{dt} \end{bmatrix} = \begin{bmatrix} \left[\left(\dfrac{-r_L}{L} \right) - \left(\dfrac{(1-d)^2 (R_{LED} r_c)}{L(R_{LED} + r_c)} \right) \right] & \dfrac{-R_{LED}(1-d)}{L(R_{LED} + r_c)} \\ \dfrac{R_{LED}}{C(R_{LED} + r_c)} & \dfrac{-1}{C(R_{LED} + r_c)} \end{bmatrix} \begin{bmatrix} i_L \\ v_c \end{bmatrix} + \begin{bmatrix} \dfrac{1}{L} \\ 0 \end{bmatrix} v_{in}$$

(17)

$$v_o = \begin{bmatrix} \dfrac{(1-d)R_{LED} r_c}{(R_{LED} + r_c)} & \dfrac{R_{LED}}{(R_{LED} + r_c)} \end{bmatrix} \begin{bmatrix} i_L \\ v_c \end{bmatrix}$$

(18)

Using standard linearization techniques and introducing perturbations as $v_{in} = V_{in} + \hat{v}_{in}$, $i_L = I_L + \hat{i}_L$, $v_c = V_c + \hat{v}_c$, $d = D + \hat{d}$, $v_o = V_o + \hat{v}_o$ as follows:

$$L \frac{d(I_L + \hat{i}_L)}{dt} = (V_{in} + \hat{v}_{in}) - r_L (I_L + \hat{i}_L) - (1 - D - \hat{d})(V_o + \hat{v}_o)$$

(19)

$$C \frac{d(V_C + \hat{v}_c)}{dt} = \frac{(1 - D - \hat{d})R_{LED}}{(R_{LED} + r_c)} (I_L + \hat{i}_L) - \frac{(V_c + \hat{v}_c)}{(R_{LED} + r_c)}$$

(20)

$$V_o + \hat{v}_o = \frac{(1 - D - \hat{d})R_{LED} r_c}{(R_{LED} + r_C)} (I_L + \hat{i}_L) + \frac{R_{LED}(V_c + \hat{v}_c)}{(R_{LED} + r_c)}$$

(21)

Seperating terms of $\hat{i}_L$, $\hat{v}_c$, $\hat{v}_{in}$ and $\hat{d}$, the small signal model of the system would be like:

$$\begin{bmatrix} \dfrac{d\hat{i}_L}{dt} \\ \dfrac{d\hat{v}_c}{dt} \end{bmatrix} = \begin{bmatrix} \left[\left(\dfrac{-r_L}{L} \right) - \left(\dfrac{(1-D)^2 (R_{LED} r_c)}{L(R_{LED} + r_c)} \right) \right] & \dfrac{-(1-D)R_{LED}}{L(R_{LED} + r_c)} \\ \dfrac{(1-D)R_{LED}}{C(R_{LED} + r_c)} & \dfrac{-1}{C(R_{LED} + r_c)} \end{bmatrix} \begin{bmatrix} \hat{i}_L \\ \hat{v}_c \end{bmatrix} + \begin{bmatrix} \dfrac{1}{L} & \left[\left(\dfrac{V_o}{L} \right) + \left(\dfrac{(1-D)R_{LED} r_c I_L}{L(R_{LED} + r_c)} \right) \right] \\ 0 & \dfrac{-R_{LED} I_L}{C(R_{LED} + r_c)} \end{bmatrix} \begin{bmatrix} \hat{v}_{in} \\ \hat{d} \end{bmatrix}$$

(22)

$$v_o = \begin{bmatrix} \dfrac{(1-D)R_{LED} r_c}{(R_{LED} + r_c)} & \dfrac{R_{LED}}{(R_{LED} + r_c)} \end{bmatrix} \begin{bmatrix} \hat{i}_L \\ \hat{v}_c \end{bmatrix} + \begin{bmatrix} 0 & \dfrac{-I_L R_{LED} r_c}{(R_{LED} + r_c)} \end{bmatrix} \begin{bmatrix} \hat{v}_{in} \\ \hat{d} \end{bmatrix}$$

(23)

The ac small signal control to inductor current open loop transfer function can be obtained by simply solving the matrix i.e:

$$\frac{\hat{i}_L(s)}{\hat{d}(s)} = \frac{V_o(R_{LED} + 2r_c)}{L(R_{LED} + r_c)} \left(\frac{s + \dfrac{1}{C\left(\dfrac{R_{LED}}{2} + r_c\right)}}{s^2 + \dfrac{C\left(r_L(R_{LED} + r_c) + R_{LED}r_c(1-D)^2\right) + L}{LC(R_{LED} + r_c)} s + \dfrac{(1-D)^2 R_{LED} + r_L}{LC(R_{LED} + r_c)}} \right) \quad (24)$$

4. Results and Analysis

To demonstrate the derived state-space model, a boost converter with switching frequency $F_S = 50kHz$, $V_{in} = 12V$, $D = 0.6$, $L = 285\mu H$, $r_L = 0.15\Omega$, $C = 76\mu F$, $r_C = 0.3\Omega$ is simulated using MATLAB simulation environment. Votage drop in both the switches is considered almost neglible as the input voltage is much greater than it. For load an automotive headlamp with 8 *LUXEON Rebel ES* high brightness LEDs connected in series configuration is considered, having $R_{LED} = 34\Omega @ I_F = 700mA$. Figure 7 and Figure 8 show the bode diagrams and open-loop step response respectively. These plots can be further used in designing of a robust feed-back control network and will be discussed in future work.
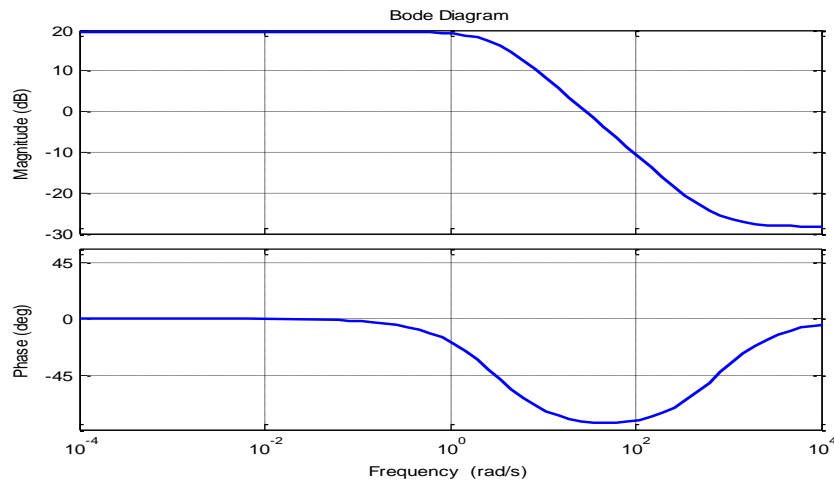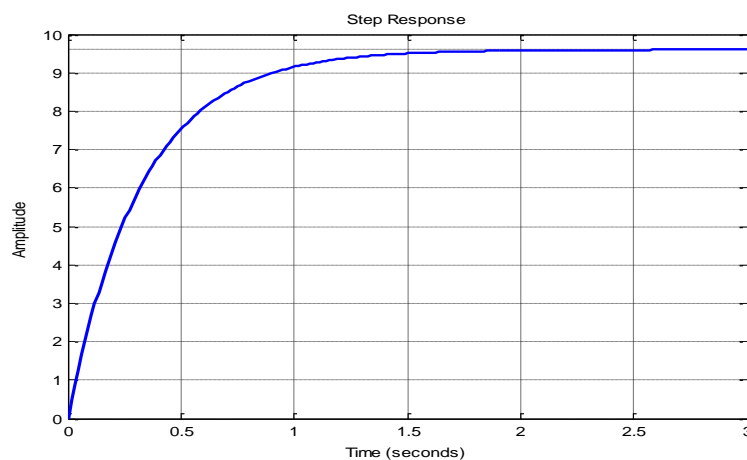

Figure 7. Magnitude and phase plots

Figure 8. Step response

5. Conclusion

This paper presents dynamic behavior modeling of a boost type dc-dc converter for high-brightness LED (HBLED) driving applications. The steady state operation in the presence of all system parasitics has been discussed to derive ac small signal control to output current open-loop transfer function for continuous conduction mode (CCM). The derived transfer function will be further used in modeling design process of current-mode controlled feed-back system. Finally, frequency and transient responses have been shown using MATLAB simulation environment confirming the validity of derived transfer function within the designed parameters. To conclude, this work introduced a systematic method for deriving and simplifying averaged circuit models for pulse width modulated swithing power converters for high-brightness LED applications.

Acknowledgment

References

[1] H-H Chou, Y-S Hwang, J-J Chen. An Adaptive Output Current Estimation Circuit for A Primary-Side Controlled LED Driver. *IEEE Transactions on Power Electronics.* 2013; 28: 4811-4819.
[2] C-B Park, B-H Choi, J-P Cheon, C-T Rim. Robust Active LED Driver with High Power Factor and Low Total Harmonic Distortion Compatible with A Rapid-Start Ballast. *Journal of Power Electronics.* 2014; 14: 226-236.
[3] K Loo, W-K Lun, S-C Tan, Y Lai, CK Tse. On Driving Techniques for LEDs: Toward A Generalized Methodology. *Power Electronicszz IEEE Transactions on. 2009;* 24: 2967-2976, 2009.
[4] X Wu, C Hu, J Zhang, C Zhao. Series–Parallel Autoregulated Charge-Balancing Rectifier for Multioutput Light-Emitting Diode Driver. *IEEE Transactions on Industrial Electronics.* 2014; 61: 1262-1268.
[5] X Wu, C Hu, J Zhang, Z Qian. Analysis and Design Considerations of LLCC Resonant Multioutput DC/DC LED Driver with Charge Balancing and Exchanging of Secondary Series Resonant Capacitors. *IEEE Transactions on Power Electronic. 2015;* 30: 780-789.
[6] Y Wang, S Gao, Y Guan, J Huang, D Xu, W Wang. A Single-Stage LED Driver Based on Double LLC Resonant Tanks for Automobile Headlight With Digital Control. *IEEE Transactions on Transportation Electrification.* 2016; 2: 357-368.
[7] L Corradini, G Spiazzi. A High-Frequency Digitally Controlled LED Driver for Automotive Applications with Fast Dimming Capabilities. in *Energy Conversion Congress and Exposition (ECCE), 2013 IEEE,* 2013: 3110-3117.
[8] MY Hariyawan, R Hidayat, E Firmansyah. The Effects of Spread-Spectrum Techniques in Mitigating Conducted EMI to LED Luminance. *International Journal of Electrical and Computer Engineering.* 2016; 6: 1332.
[9] S Winder. *Power supplies for LED driving*: Newnes. 2011.
[10] MK Kazimierczuk. *Pulse-Width Modulated DC-DC Power Converters*: John Wiley & Sons. 2015.
[11] S Bacha, I Munteanu, AI Bratcu. Power Electronic Converters Modeling and Control. *Advanced Textbooks in Control and Signal Processing.* 2014: 454.
[12] FA Silva. Power Electronics and Energy Conversion Systems. Vol, 1: Fundamentals and Hard-Switching Converters [Book News]. *IEEE Industrial Electronics Magazine,* 2014; 8: 66-67.
[13] A Ioinovici. *Fundamentals and Hard-Switching Converters*: John Wiley & Sons, 2013.
[14] R Ramya, K Selvi. State Space Modeling and Small Signal Stability Analysis of Synchronous Generator with Fuzzy based AVR. *International Journal of Electrical and Computer Engineering.* 2012; 2: 798, 2012.
[15] J Wang, Y Cai, X Li, X Zhao, C Zhang. Design of Automotive Headlamp with high-power LEDS. *International Journal of Automotive Technology.* 2014; 15: 673-681.
[16] M Louzazni, EH Aroudam, H Yatimi. Modeling and Simulation of A Solar Power Source for A Clean Energy without Pollution. *International Journal of Electrical and Computer Engineering.* 2013*;* 3: 568.